Available online at www.sciencedirect.com

ScienceDirect

Procedia Engineering 00 (2016) 000–000

Procedia Engineering

www.elsevier.com/locate/procedia

1st International Conference on the Material Point Method, MPM 2017

Studying hydraulic failure in excavations using two-phase material point method

Farzad Fatemizadeh[a,*], Dieter F. Stolle[b], Christian Moormann[a]

[a]*Institute of Geotechnical Engineering, University of Stuttgart, Pfaffenwaldring 35, 70569 Stuttgart, Germany*
[b]*McMaster University, 1280 Main Street West, Hamilton, Ontario, Canada*

Abstract

The head difference between the inside and outside of an excavation leads to seepage flow into the excavation. High seepage velocities lead to high seepage pressures that decrease the effective stresses. In extreme cases, the soil fluidizes and cannot sustain the seepage forces, which causes the soil-water mixture to flow into the excavation site.
The problem of hydraulic failure is simulated using the Material Point Method (MPM). The ability of MPM to simulate this phenomenon is shown and some concluding remarks are presented.

Peer-review under responsibility of the organizing committee of the 1 st International Conference on the Material Point Method.

Keywords: material point method; soil-water interaction; excavations; seepage forces; failure.

1. Introduction

It is not uncommon during construction to encounter situations in which the bottom of an excavation is well below the groundwater table. This often requires lowering the water level that results in a decrease of the head of water inside the excavation. The head difference between the inside and outside of the excavation leads to seepage into the excavation. The retaining structures for the excavation, such as e.g. a cofferdam, together with a dewatering system are responsible to control the resulting seepage forces. Due to unknowns in site conditions, or flawed construction, unexpected increases in the pore pressure can develop that further decrease the effective stresses at the

* Corresponding author.
E-mail address: farzad.fatemizadeh@igs.uni-stuttgart.de

Peer-review under responsibility of the organizing committee of the 1 st International Conference on the Material Point Method.

base of the excavation, which in turn may result in a fluidized soil. This phenomenon is less critical in soil types with high values of hydraulic conductivity like gravel, but in soil types with smaller values for hydraulic conductivity like well graded sand becomes important. The fluidized soil cannot withstand any load and the soil-water mixture may flow into the excavation site, which can lead to a complete failure of the retaining system. Numerical modelling of such cases may help to understand the phenomenon and to avoid such catastrophic incidents.

Numerical modelling of hydraulic failure is a complex task, in which the water-soil interaction, including the possibility of fluidization and sedimentation of the soil particles, must be taken into account. The initiation of the failure can be simulated using the standard finite element method (FEM) (cf. [1] & [2]), but to study the post failure behaviour, advanced numerical models that are capable of simulating large deformations of saturated soil are required.

In this study, the Material Point Method (MPM) is adopted to simulate hydraulic failure in excavations. MPM is a numerical procedure that accommodates large deformations and avoids the mesh distortion problem that is common with the classical FEM method. The effectiveness of this method in soil mechanics for simulating large deformations has been addressed by different researchers. MPM has been successfully applied to model fully saturated soil in a variety of examples; see e.g. Al-Kafaji [3], Bandara [4] as well as Więckowski [5] and Vermeer et al. [6]. Al-Kafaji [3] used the velocity-velocity formulation with single set of material points to represent the soil-water mixture with separated velocity fields for each phase. He studied the wave attack on a sea dike. Bandara [4] used the displacement-displacement formulation with two different sets of material points to represent the soil and water phases separately. She studied the levee failure due to water seepage. Więckowski [5] investigated the erosion of a slope attacked by water. He also used two sets of particles and considered the effect of porosity change in his formulation and used a criterion to define the fluidization of solid particles. Vermeer et al. [6] used the same formulation and studied the collapse of a submerged soil column considering the fluidization and sedimentation of the soil particles.

Other numerical methods are also adopted to investigate the hydraulic heave in excavations, e.g. Grabe and Stefanova [7] used the Smooth Particle Hydrodynamics (SPH) method in their study. This phenomenon is also investigated experimentally by different researchers e.g. Alsaydalani and Clayton [8] and Zoueshtiagh and Merlen [9].

The objective of this paper is to address two necessary aspects required for numerically modelling hydraulic failure in excavations, namely the ability to represent large deformations and to formulate two-phase interactions (including free water, saturated soil, fluidization and sedimentation). The structure of this paper is as follows: Section 2 introduces the two-phase formulation used to describe the fully saturated soil in MPM, which is followed by a simple validation example of a one-dimensional consolidation problem. In Section 3, the Lagrangian formulation for free water is introduced and validated by solving the Poiseulle flow problem, for which an analytical solution exists. In Section 4, the problem of hydraulic failure is simulated and Section 5 provides some concluding remarks.

2. Two-phase formulation of fully saturated soil in MPM

Based on Zienkiewicz and Shiomi [10], the *u-U* formulation, in which displacement of solid (*u*) and displacement of water (*U*) are the primary variables, is chosen to describe the behavior of fully saturated soil. This is due to the fact that, in the *u-U* formulation mapping the pressure as an intensive thermodynamic property between the particles which carry all the state variables and nodes of the background mesh is excluded [3]. Two material point sets are used to represent the solid and fluid phases separately. This is done in order to enable the implementation of free water in the developed program. The starting point is the momentum balance equations of the fluid (1) and fluid-solid mixture (2), from which the displacement (velocity) field of the fluid and solid phases can be calculated, respectively:

$$n\rho_w \frac{d\hat{w}_j}{dt} = n\frac{\partial p}{\partial x_j} + n\rho_w g_j - \frac{n^2 \rho_w g}{k}\left(\hat{w}_j - \hat{v}_j\right) \tag{1}$$

$$(1-n)\rho_s \frac{d\hat{v}_j}{dt} + n\rho_w \frac{d\hat{w}_j}{dt} = \frac{\partial \sigma_{ij}}{\partial x_j} + \rho_{sat} g_j . \tag{2}$$

Here ρ_w is the density of the water, ρ_s corresponds to the soil grain density, ρ_{sat} denotes the saturated density, $\hat{w}_j$ is the velocity of the water phase and p is the water pressure, g_j represents the gravitational acceleration vector, n is the porosity, k is the permeability, $\hat{v}_j$ is the velocity of the solid phase and σ_{ij} is the total stress tensor. It should be noted that the porosity is updated in time and space and is not a constant value. During the derivation of weak form of equation (1), after applying the integration by parts and Green's theorem to the first term on the right hand side:

$$\int_\Omega \hat{t}_j n \frac{\partial p}{\partial x_j} d_\Omega = \int_\Omega \frac{\partial}{\partial x_j}\left[\hat{t}_j n p\right] d_\Omega - \int_\Omega \frac{\partial}{\partial x_j}\left[\hat{t}_j n\right] p d_\Omega = \int_\Omega \hat{t}_j n \bar{p}_j d_S - \int_\Omega \frac{\partial \hat{t}_j}{\partial x_j} n p d_\Omega - \int_\Omega \frac{\partial n}{\partial x_j} \hat{t}_j p d_\Omega \tag{3}$$

the gradient of the porosity appears in the last term in right hand side of equation (3) which needs to be considered as well. Here $\hat{t}_j$ is the weighting function, Ω is the current domain, $\bar{p}$ is the pressure applied at the boundary and S is the boundary of the domain on which the pressure of the fluid is prescribed. The calculation of this term is discussed thoroughly by Więckowski [11].

Taking into account the mass conservation equation of the water and solid phases, the storage equation is derived. It is used to calculate the pressure in the water:

$$\frac{dp}{dt} = \frac{K_w}{n}\left[(1-n)\frac{d\hat{v}_j}{dx_j} + n\frac{d\hat{w}_j}{dx_j}\right] \tag{4}$$

with K_w representing the bulk modulus of the water. The effective stresses are calculated in the usual way by relating the stress rates to the strain rates of the soil skeleton:

$$\dot{\sigma}'_{ij} = D_{ijkl}\dot{\varepsilon}_{kl} \tag{5}$$

where D_{ijkl} is the constitutive tensor and $\dot{\varepsilon}_{kl}$ and $\dot{\sigma'}_{ij}$ are the strain and stress rate tensors respectively.

After transforming equations (1) and (2) to the weak form and discretizing them, they can be solved using appropriate initial and boundary conditions. Explicit (which is used in this study) or implicit time integration schemes can be adopted. The whole solution process and derivation of the equations discussed in detail in [4].

To validate the presented formulation we consider one-dimensional consolidation for which an analytical solution exists. A fully saturated linear elastic soil column of 1 m thickness supports a surface traction of 10 kPa and has a permeability of 10^{-3} m/s and porosity of 0.4. The elastic modulus of the soil skeleton is 10 MPa and the bulk modulus of the water is 300 MPa. A smaller value for the bulk modulus of the water than its physical one is chosen in order to increase the time step size needed for the explicit time integration scheme. The dry density of the soil is 1600 kg/m^3 and the water density is 1000 kg/m^3. The soil layer is discretized with 50 layers of linear triangular elements, with each containing one water and one solid material point. An initial excess pore water pressure of 10 kPa is assumed. Fig. 1 shows the pore pressure as a function of depths for different normalised time

$$T = \frac{kE_s t}{\gamma_w D^2} . \tag{6}$$

Here k is the permeability and E_s is the elastic modulus of the soil skeleton, γ_w is the specific weight of the water, t is the time and D is the length of the drainage path. A good agreement between the analytical and numerical results is apparent. Small oscillations at the dimensionless time of 0.05 are attributed to the wave reflections from the boundary.

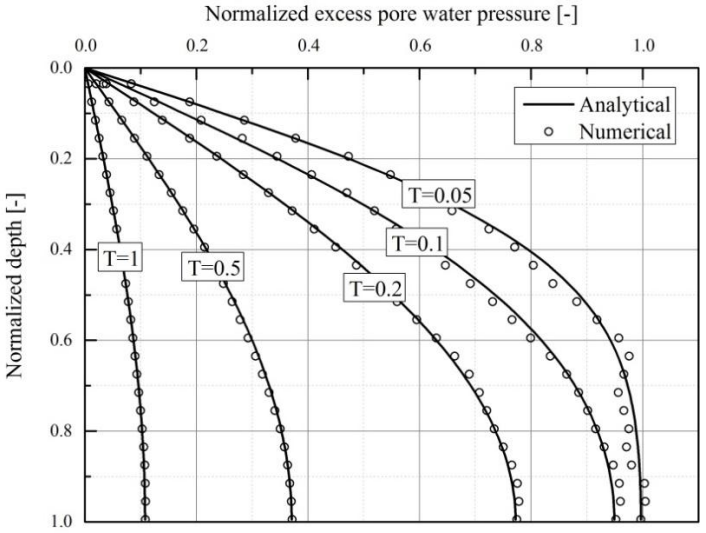

Fig. 1. Analytical and numerical results of the one dimensional consolidation example.

3. Formulation of free water in MPM

In order to simulate the nearly incompressible free water (water which is not in the pores of the solid) in MPM, the starting point is the momentum balance equation of fluid:

$$\rho_w \frac{d\hat{w}_j}{dt} = \frac{\partial \sigma^w{}_{ij}}{\partial x_j} + \rho_w g_j \tag{7}$$

where $\sigma^w{}_{ij}$ is the stress tensor for the fluid. The displacement field of the fluid phase is calculated via equation (7). We determine the fluid pressure by considering the mass balance equation of the fluid:

$$\frac{1}{\rho_w}\frac{d\rho_w}{dt} + \frac{\partial w_i}{\partial x_i} = 0. \tag{8}$$

By adopting the constitutive law for the fluid:

$$\sigma^w{}_{ij} = -p\delta_{ij} + 2\mu\dot{\varepsilon}^w{}_{ij} \tag{9}$$

we can calculate the stress in the water where δ_{ij} is the Kronecker delta, μ is the viscosity and $\dot{\varepsilon}^w{}_{ij}$ is the strain rate tensor of the fluid. To solve the complete system of equations, equation (7) is transformed to its weak form and then discretized in the domain. It is solved using initial and boundary conditions and appropriate time integration scheme (here explicit time integration scheme). The complete formulation and solving procedure are described in [12] where the formulation is also adopted and validated for problems including large deformations.

It should be noted that equation (1) can be used for the free water by setting the last term in right hand side (drag force) to zero. Then by implementing the two-phase formulation with two sets of material points for the water and solid phases separately, free water can be taken into account automatically.

To validate the formulation presented here, the Poiseulle laminar flow problem [12] is simulated and the results are compared with the analytical solution. In this example, a pressure gradient of 40 kPa is applied on the water in a

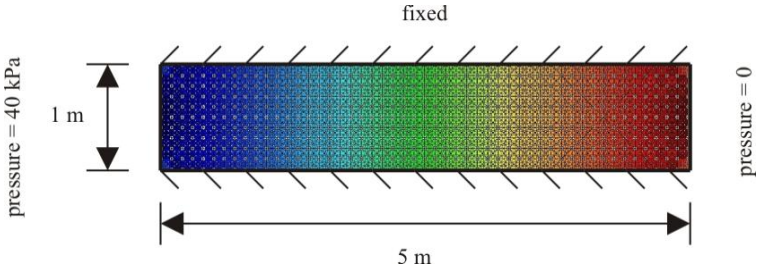

Fig. 2. Geometry and pressure distribution of the Poiseulle flow example.

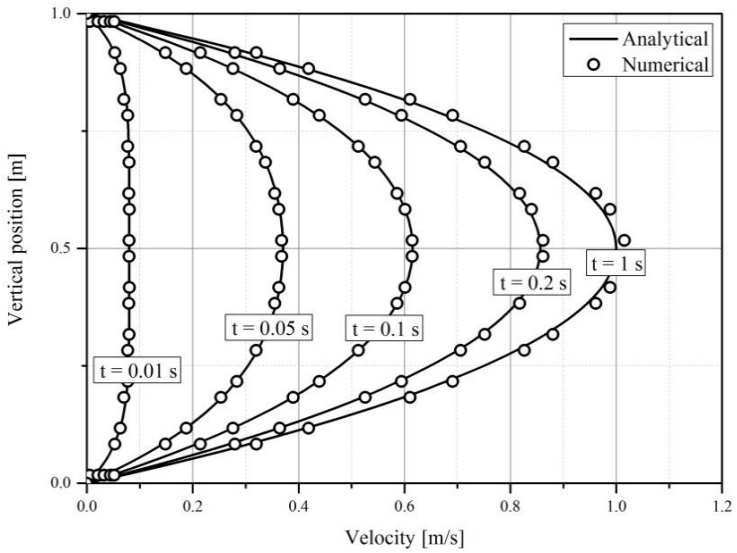

Fig. 3. Analytical and numerical results of the Poiseulle flow example.

pipe that has a length of 5 m and height of 1 m (Fig. 2) and the gravitational acceleration is ignored. Water has a bulk modulus of 20 GPa and viscosity of 1 Pa.s. A larger value for the bulk modulus of the water is chosen to capture the analytical solution which is derived for an incompressible fluid and the viscosity is also a larger value in order to have a laminar flow. The position of the material points are kept constant during the simulation. The profile of the velocity for different times is then considered and the results are compared to the analytical solution (Fig. 3). It is observed that good agreement exists between the analytical and numerical results. It should be noted that pressure is introduced as a natural boundary condition. Fig. 2 shows the variation in pressure.

4. Numerical simulation of hydraulic failure in excavations using MPM

After implementing the fully saturated soil and free water in MPM, they can be combined together to solve problems which involve the interaction of water and soil in fully saturated conditions, such as the hydraulic failure in excavations. The geometry of the model under consideration is shown in Fig. 4. The geometry is chosen in a way that it can be used later together with experimental investigations of the problem under study. The model contains a permeable filter plate with a thickness of 0.02 m and a soil layer with a thickness of 0.2 m, which has 0.15 m water on top.

The linear elastic filter plate has an elastic modulus of 20 MPa, Poisson's ratio of 0.3, porosity of 0.4 and permeability of 0.01 m /s. The cohesionless soil has a solid grain density of 2500 kg/m^3, elastic modulus of 20 MPa,

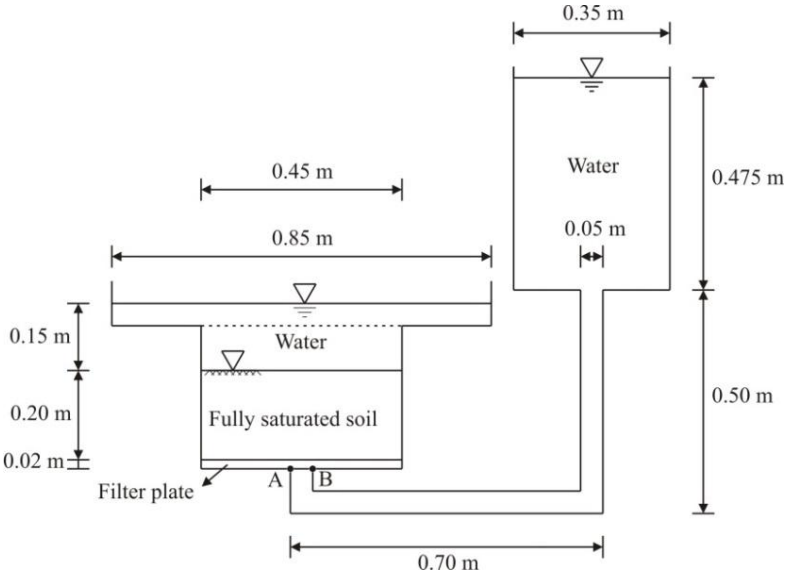

Fig. 4. Geometry of the hydraulic failure model under consideration.

Poisson's ratio of 0.3, porosity of 0.4, permeability of 0.001 m/s and friction angle of 35°. The elastic-perfectly plastic Mohr-Coulomb material model is used for the soil. Water has a bulk modulus of 2 GPa and viscosity of 0.001 Pa.s.

For the simulation, linear triangular elements with three solid and four water particles per element in the fully saturated soil part and 10 water particles per element in the pure fluid part are used. A finer mesh is adopted for the soil water mixture part to capture the behavior of the soil more accurately. The pipe at position AB is initially closed until the system reaches the hydrostatic equilibrium. Then it is opened. The pore water pressure in the soil begins to increase with the effective stresses decreasing. The necessary pore pressure difference between the top and bottom of the soil sample to cause the hydraulic failure is estimated via:

$$F_s = \frac{i_c}{i_m} = \frac{\gamma'/\gamma_w}{\Delta h/L} = 1 \;\rightarrow\; \frac{\Delta h}{L} = \frac{\gamma'}{\gamma_w} \;\rightarrow\; \Delta h = \frac{\gamma'}{\gamma_w} L \;\rightarrow\; \frac{\Delta u_w}{\gamma_w} - L = \frac{\gamma'}{\gamma_w} L \tag{10}$$

$$\Delta u_w = (\gamma' + \gamma_w) L = \gamma_{sat} L = 2050 kg/m^3 \times 10 m/s^2 \times 0.22 m = 4510 Pa$$

which is less than the applied pressure difference 5050 Pa (the difference between the water levels). In equation (7) F_s is the safety factor, i_c is the critical hydraulic gradient, i_m is the available hydraulic gradient, L is the thickness of the soil, Δh is the head difference and Δu_w is the pore water pressure difference between the top and bottom of the soil sample and γ', γ_w and γ_{sat} are the specific buoyant, water and saturated weights, respectively.

When the soil is fluidized the effective stresses approach zero and the surface heaves due to the upward drag caused by the seepage pressure. When this happens, the whole system loses stability and failure occurs. Fig. 5 shows the total deformation of the soil material points 0.3 s (a) and 1.0 s (b) after opening the AB gage. As can be seen in Fig. 5 (a), a small fluidized zone above the injection area is firstly built which is called the transitional state [9] before the total failure happens. Based on Zoueshtiagh and Merlen [9] the transition state is a stable state and by adjusting the water level in the tank a stable situation with a small fluidized zone can be achieved. By continuing the simulation, the fluidized zone expands and the total failure happens [9]. Water particles are not shown here, as the focus is on the deformation of the soil. Fig. 6 illustrates the soil mass concentration mapped on the nodes of the background mesh at 0.3 s (a) and 1.0 s (b) after opening the AB gage. The mapping is done based on [10]:

$$\rho_i = \frac{\sum_{j=1}^{n_p}\sum_{p=1}^{p_j} N_{i(x_p)} M_p}{\sum_{j=1}^{n_p} A_j / 3} \tag{11}$$

where ρ_i is the mass concentration of the node i, n_p is the number of elements connected to the node i containing at least one material point, p_j is the number of material points located in the jth element, $N_{i(x_p)}$ is the shape function of node i at the position of particle p, M_p is the mass of particle p and A_j is the area of element j. As illustrated in Fig. 6 (a), the soil mass concentration decreases from the initial value of 1500 kg/m^3:

$$\rho = (1-n)\rho_s = (1-0.4)\times 2500 = 1500 kg/m^3 \tag{12}$$

just above the water inlet with a small increase above this region. By the expansion of the fluidized area, the soil mass concentration also continues decreasing (Fig. 6 (b)).

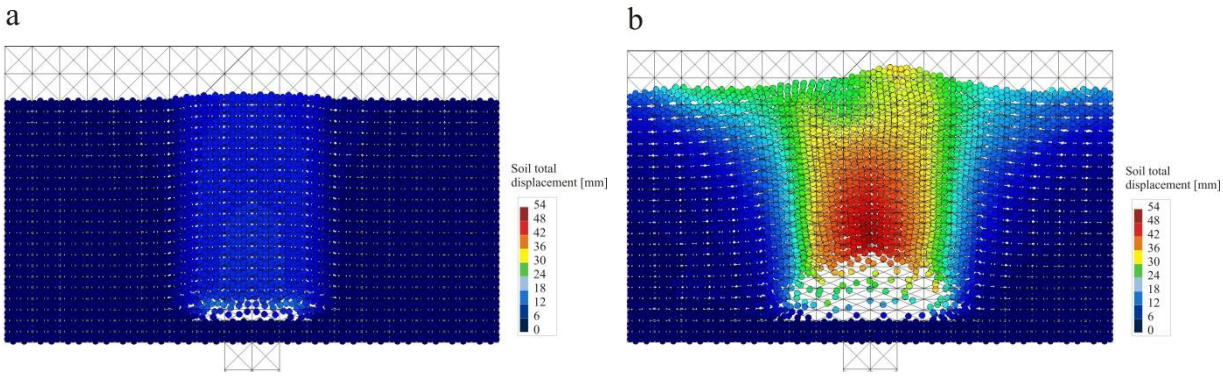

Fig. 5. Total displacement of the soil particles (a) 0.3 s and (b) 1.0 s after opening the AB gage.

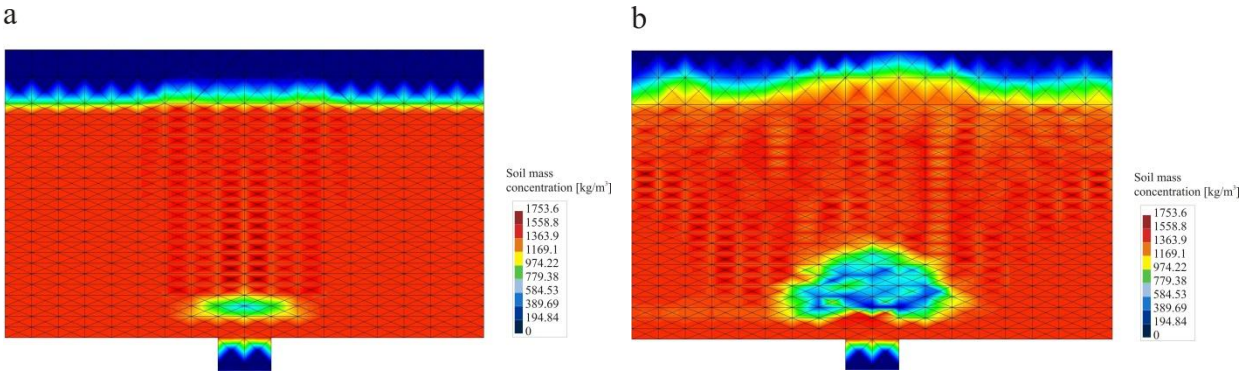

Fig. 6. Soil mass concentration mapped on the nodes (a) 0.3 s and (b) 1.0 s after opening the AB gage.

5. Conclusions and future work

The formulation of two-phase MPM was mentioned for fully saturated soil and validated using a simple one-dimensional consolidation example. Then the formulation for the water using the Navier-Stokes equations was mentioned and validated using the Poiseulle flow problem. Having both implementations in hand, they were combined to solve the soil and free water interaction problem that considered hydraulic failure. This problem was simulated using an in-house MPM program.

As in this study only the effective stresses are considered for detection of the fluidized solid material points, in the next steps more accurate conditions need to be investigated and adopted in the formulation. More advanced constitutive models and higher order shape functions will be adopted to have a better understanding of the soil behavior.

References

[1] N. Benmebarek, S. Benmebarek, R. Kastner, Numerical studies of seepage failure of sand within a cofferdam, *Comput Geotech*, 32 (2005) 264-273.
[2] S. Koltuk & R. Iyisan, Numerical Analysis of Groundwater Flow Through a Rectangular Cofferdam, *EJGE*, 18 (2013) 2041-2052.
[3] I.K.J. Al-Kafaji, Formulation of a Dynamic Material Point Method (MPM) for Geomechanical Problems, PhD thesis, Institute of Geotechnical Engineering, University of Stuttgart, 2013.
[4] S.S. Bandara, Material Point Method to simulate Large Deformation Problems in Fluid-saturated Granular Medium, PhD thesis, University of Cambridge, 2013.
[5] Z. Więckowski, Two-phase numerical model for soil-fluid interaction problems, Proceedings of the 3rd international symposium on computational geomechanics (COMGEO III), Karkow, Poland (2013) 410-419.
[6] P.A. Vermeer, L. Sittoni, L. Beuth, Z. Więckowski, Modeling soil-fluid and fluid-soil transitions with applications to tailings, Tailings and Mine Waste, Alberta, Canada, (2013) 305-315.
[7] J. Grabe & B. Stefanova, Numerical modeling of saturated soils based on smoothed particle hydrodynamics (SPH) Part2: Coupled analysis, *Bautechnik*, 38 (2015) Heft 3, 218-229.
[8] M.O.A. Alsaydalani & C.R.I. Clayton, Internal fluidization in granular soils, *J. Geotech. Geoenviron. Eng.*, 140 Issue 3 (2014).
[9] F. Zoueshtiagh & A. Merlen, Effect of a vertically flowing water jet underneath a granular bed, *Physical review*, 75, 056313 (2007).
[10] O.C. Zienkiewicz & T. Shiomi, Dynamic behaviour of saturated porous media; the generalized Biot formulation and its numerical solution, *Int. J. Numer. Anal. Methods Geomech*, 8 (1984) 71-96.
[11] Z. Więckowski, Enhancement of the Material Point Method for fluid-structure interaction and erosion, Report on EU-FP7 research project Geo Fluid PIEF-GA-2010-274335.
[12] F.M. Hamad, Formulation of a Dynamic Material Point Method and applications to soil-water-geotextile systems, PhD thesis, Institute of Geotechnical Engineering, University of Stuttgart, 2014.